Mugla Journal of Science and Technology

COMPARISON OF WIND-SPEED DISTRIBUTIONS UNDER A UNIFIED TURBINE FRAMEWORK: A PLANT-LEVEL POWER ANALYSIS

Murat OZKUT*, Department of Mathematics, University of Economics, Türkiye, murat.ozkut@ieu.edu.tr
(https://orcid.org/ 0000-0002-0699-892X)

Received: 06.09.2025, Accepted: 05.12.2025
*Corresponding author
Research Article
DOI: 10.22531/muglajsci.1779320

Abstract

This paper presents a comparative framework for translating alternative wind-speed distributions into plant-level power and reliability metrics under a unified turbine framework. We compare three widely used distributions—Weibull, Gamma, and Birnbaum-Saunders (BS)—while keeping all engineering inputs fixed (turbine power curve, rated power, operational speeds, and availability p). For each distribution, we construct the single-turbine power distribution, incorporate availability, and obtain the aggregate plant distribution for N turbines via discrete convolution. Our analysis reveals that distributional choice substantially affects sizing predictions: Birnbaum-Saunders consistently yields the most conservative estimates, requiring 30–70% more turbines than Weibull to achieve equivalent reliability targets across tested scenarios. Weibull provides the most optimistic predictions, while Gamma occupies an intermediate position. These differences are most pronounced at mid-range capacity thresholds (2–7 MW for $N = 10$), where practical planning decisions occur. For moderate reliability targets, distribution choice alone can shift minimum fleet size requirements by 2–4 turbines, with direct implications for capital investment and risk assessment. We provide sensitivity analyses, mean power comparisons, and implementation details to ensure reproducibility.

Keywords: Wind-speed distributions, Weibull distribution, Gamma distribution, Birnbaum-Saunders distribution, Wind-plant reliability, Exceedance probability

BİRLEŞİK TÜRBİN ÇERÇEVESİNDE RÜZGAR HIZI DAĞILIMLARININ KARŞILAŞTIRILMASI: SANTRAL ÖLÇEĞİNDE GÜÇ ANALİZİ

Özet

Bu makale, alternatif rüzgar hızı dağılımlarını birleşik türbin çerçevesi altında santral düzeyindeki güç ve güvenilirlik ölçütlerine dönüştürmek için karşılaştırmalı bir çerçeve sunmaktadır. Tüm mühendislik girdileri sabit tutularak (türbin güç eğrisi, nominal güç, işletme hızları ve kullanılabilirlik p), üç yaygın dağılım-Weibull, Gamma ve Birnbaum-Saunders (BS)-karşılaştırılmıştır. Her dağılım için tek türbin güç dağılımı oluşturulmuş, kullanılabilirlik etkisi dâhil edilmiş ve ayrık konvolüsyon yöntemiyle N adet türbinin toplam tesis güç dağılımı elde edilmiştir. Analiz sonuçları, dağılım seçiminin boyutlandırma tahminlerini önemli ölçüde etkilediğini ortaya koymaktadır: Birnbaum–Saunders dağılımı, test edilen senaryolar boyunca en muhafazakâr tahminleri üretmekte ve Weibull dağılımına kıyasla aynı güvenilirlik hedeflerine ulaşmak için %30-70 oranında daha fazla türbin gerektirmektedir. Weibull dağılımı en iyimser tahminleri sağlarken, Gamma dağılımı arada bir konumda yer almaktadır. Bu farklılıklar, planlama açısından kritik olan orta aralık kapasite eşiklerinde ($N = 10$ için 2-7 MW) en belirgin düzeydedir. Orta düzey güvenilirlik hedefleri için, yalnızca dağılım seçimi minimum filo boyutu gereksinimini 2-4 türbin arasında değiştirebilmekte ve bu durum sermaye yatırımı ile risk değerlendirmesi açısından doğrudan etkiler yaratmaktadır. Çalışmada ayrıca duyarlılık analizleri, ortalama güç karşılaştırmaları ve tekrarlanabilirliği sağlamak amacıyla uygulama ayrıntıları sunulmaktadır.

Anahtar Kelimeler: Rüzgar hızı dağılımları, Weibull dağılımı, Gamma dağılımı, Birnbaum-Saunders dağılımı, Rüzgar santrali güvenilirliği, Aşma olasılığı

Cite

Ozkut, M., (2025). "Comparison of Wind-Speed Distributions for Analyzing Plant-Level Wind Power", Mugla Journal of Science and Technology, 11(2), 118-126.

1. Introduction

Wind energy is expanding rapidly; however, plant-level output is highly variable due to the stochastic nature of wind speed. This variability propagates directly to electrical production, making probabilistic modeling indispensable for planning, reliability assessment, and risk-aware operation. Two major threads anchor the literature: dynamic wind-speed modeling and probabilistic forecasting of power. On the dynamic side, continuous wind-speed models based on stochastic differential equations have been proposed in [1]. On the

forecasting side, probabilistic predictive densities for aggregated wind power across multiple farms are developed in [2], particle-filter-based aggregated forecasting is presented in [3], and probabilistic forecasts have been integrated into gas-unit scheduling in [4]. Data-driven learning has also been explored; wind-power estimation with recurrent neural networks has been reported in [5].

A large empirical body fits parametric/nonparametric distributions to wind speed from many sites. Long-term hourly records have been analyzed with Weibull, Rayleigh, lognormal, normal, and gamma laws (Rwanda study, [6]). Regional assessments emphasize identifying the best-fit distribution for wind-resource characterization (Malaysia, [7]). Nonparametric approaches improve probabilistic wind-power forecasting ([8]). Comparative multi-site evaluations show that the preferred distribution depends on regime ([9]). The Birnbaum–Saunders (BS) family originating in fatigue mechanics has also been advocated for wind-speed/power modeling ([9]).

Beyond fitting wind speed, several works examine theoretical wind-power distributions. A derivation of wind-power probability density functions (PDFs) from first principles is given in [10], statistical characteristics of aggregated wind power are analyzed in [11], and plant-level power distributions incorporating turbine availability are developed in [12].

Recent studies have advanced wind-speed distribution modeling using sophisticated statistical techniques. In [13], Weibull parameter estimation methods have been enhanced for complex terrain conditions. A neutrosophic BS model has been proposed for imprecise wind data in [14]. In [15], statistical analyses combined with multifractal detrended fluctuation analysis (MFDFA) characterize wind speed variations in Sichuan Province. Applications of the Champernowne distribution at Green Energy Parkin Ben Guerir have been explored in [16]. Moreover, [17] have presented probabilistic models for wind-speed prediction in Vietnam, together with data and strategies for more effective utilization of wind energy. Finally, Weibull-based energy-prediction methods have been evaluated and validated through recent case studies in [18].

Despite this progress, relatively few studies compare multiple wind-speed distributions within a single, fixed engineering pipeline keeping the turbine power curve and availability model constant and then evaluate plant-level consequences. This paper addresses that gap. We compare, rather than select, three widely used wind-speed models such as Weibull, Gamma, and BS under a common wind-to-power framework. Using a standardized piecewise turbine power curve (cut-in, rated, cut-out) and an explicit availability model, we map each wind-speed law to the single-turbine power distribution, aggregate N identical turbines to obtain the plant-level distribution $F_{\text{plant}}(x)$, and evaluate planning-relevant metrics. Given a target power threshold c_0 and minimum reliability p_0, we determine the smallest fleet size N^* such that $P\{P_{\text{plant}}>c_0\}\geq p_0$, and we report the achieved exceedance probability at N^* for each distribution. We also compare full cumulative distribution function (CDF) and mean power across the three laws over multiple $(c_0,\ p_0)$ scenarios to quantify how distributional choice holding technology and availability fixed shifts sizing recommendations and implied risk margins.

The remainder proceeds as follows: Section 2 formalizes the wind-turbine/plant model (including availability and the piecewise power curve). Section 3 details the modeling methodology and the three wind-speed laws (Weibull, Gamma, Birnbaum-Saunders), and shows how each map through the power curve to obtain plant-level distributions. Section 4 presents the numerical study and applications: exceedance-based sizing N^* for multiple $(c_0,\ p_0)$ targets, comparisons of $F_{\text{plant}}(x)$, and mean-power analyses. Section 5 summarizes the main findings and practical implications for planning and risk tolerance, and section 6 lists the references.

2. System Description

Wind speed variation is stochastic and directly impacts the power output of wind plants. This section describes the physical system associated with wind speed and its effect on power generation.

The system consists of N identical wind turbines, each characterized by a standardized piecewise power curve. The power output $\mathcal{P}_j^{WT}$ of turbine j depends on wind speed and its operational availability. It is calculated as

$$\mathcal{P}_j^{WT} = \begin{cases} 0, & \text{if } u < u_{\text{on}} \text{ or } u \geq u_{\text{off}} \\ \mathcal{P}_{rt}\dfrac{(u^3 - {u_{\text{on}}}^3)}{({u_{\text{rt}}}^3 - {u_{\text{on}}}^3)} & \text{if } u_{\text{on}} \leq u < u_{\text{rt}} \\ \mathcal{P}_{rt} & \text{if } u_{\text{rt}} \leq u < u_{\text{off}} \end{cases} \quad (1)$$

where the random variable u denotes the wind speed. In addition, the parameters u_{on}, u_{rt}, $\mathcal{P}_{rt}$ denote cut-in wind speed, rated wind speed and the rated power of a single turbine, respectively, which are given by the manufacturer. From Equation (1), it is easy to see that When wind speed falls below the cut-in speed u_{on} or exceeds the cut-out speed u_{off}, the turbine produces no electrical power. Between the cut-in speed u_{on} and the rated speed u_{rt}, turbine power output increases cubically. Power output equals the rated power $\mathcal{P}_{rt}$ when wind speed lies between the rated and cut-out speeds. If wind speed exceeds the cut-out speed, the turbine automatically shuts down to prevent mechanical damage.

In Figure 1 [2], the relationship between wind speed and the power generated by a single wind turbine is presented.

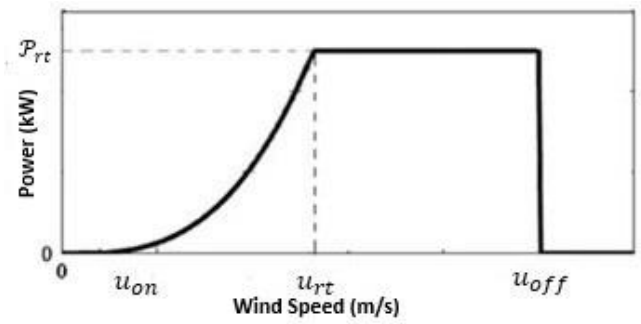

Fig.1 Piecewise power curve of a single wind turbine showing operational regimes.

Figure 1 illustrates the characteristic power curve of a single wind turbine. Variability in wind speed makes the power output $\mathcal{P}_j^{WT}$ a stochastic variable. The power curve comprises four distinct regions corresponding to specific wind speed ranges: no power generated below the cut-in and above the cut-out thresholds; cubic growth between cut-in and rated speeds; constant rated power between rated and cut-out speeds.

Wind speed is inherently variable, making the power output from a wind turbine a stochastic variable. The governing relationship can be described as follows: when wind speed falls below the switch-on threshold, the turbine does not generate electrical power because the kinetic energy in the wind is insufficient to produce output. In the range between the switch-on speed and the rated wind speed, the power output follows a cubic relationship with respect to wind velocity. Once the wind speed exceeds the rated wind speed but remains below the shut-off threshold, the turbine operates at a constant power output, denoted as $\mathcal{P}_{rt}$. If wind speeds surpass the shut-off limit, the turbine automatically deactivates to prevent mechanical failure, resulting in zero power generation.

In a wind farm comprising N independent wind turbines, the total power generated by the plant, $\mathcal{P}_N$, is the cumulative sum of the output power from each turbine:

$$\mathcal{P}_N = \sum_{j=1}^{N} \mathcal{P}_j^{WT} \tag{2}$$

In the following section, we analyze three statistical distributions widely used for modeling and fitting wind speed data: Weibull, Birnbaum-Saunders, and the two-parameter Gamma distributions.

3. Modelling methodology

This section examines various probability distributions for modeling wind speed, specifically focusing on the Weibull, Birnbaum-Saunders, and two-parameter gamma distributions. Each of these distributions is evaluated for their applicability and effectiveness in accurately representing the characteristics of wind speed data.

3.1 Probability distributions

3.1.1 Weibull distribution

The Weibull distribution is the predominant statistical function utilized in wind power applications due to its versatility and simplicity. It has proven effective in modeling a wide range of wind regimes encountered in nature. However, several studies indicate its limitations in accurately representing wind speed data, especially in scenarios characterized by high frequencies of null data, extreme low and high wind speeds, bimodal distributions, and short temporal horizons. These challenges necessitate careful consideration when applying the Weibull distribution in specific contexts.

The CDF and PDF of the two-parameter Weibull distribution are given respectively by

$$F(u) = 1 - e^{-\left(\frac{u}{\sigma}\right)^k} \tag{3}$$

and

$$f(u) = \left(\frac{k}{\sigma}\right)\left(\frac{u}{\sigma}\right)^{k-1} e^{-\left(\frac{u}{\sigma}\right)^k}, \tag{4}$$

$u \geq 0$, where the parameters k and σ denote respectively the shape and scale parameters. Unknown parameters in the Weibull distribution can be estimated from wind speed data using various methodologies, including the maximum likelihood method and the method of moments.

3.1.2 Birnbaum-Saunders distribution

The BS distribution is another statistical model commonly fitted to wind speed data. Its CDF is given by

$$F(u) = \Phi\left[\frac{1}{\varrho}\left\{\left(\frac{u}{\varsigma}\right)^{\frac{1}{2}} - \left(\frac{\varsigma}{u}\right)^{\frac{1}{2}}\right\}\right] \tag{5}$$

$u \geq 0$, where the parameters ϱ and ς denote respectively the shape and scale parameters, and Φ is the standard normal CDF.

3.1.3 Gamma distribution

The two-parameter gamma distribution (α, θ) has been effectively employed in wind speed modeling, particularly in studies focusing on low-speed wind phenomena, as noted by. Its versatility in capturing the statistical characteristics of low wind speeds makes it a valuable tool in this domain. The CDF of the two-parameter gamma distribution is given by

$$F(u) = \frac{1}{\Gamma(\alpha)\theta^{\alpha}} u^{\alpha-1} e^{-u/\theta} \tag{6}$$

where θ and α denote respectively the scale and shape parameters.

3.2 Model evaluation

Wind speed is often considered an external source of uncertainty affecting energy generation in wind power systems. In addition to this external variability, wind turbines experience internal randomness related to

their mechanical states, specifically the operational statuses of "up" (functional) and "down" (non-functional due to failure). We assume that at any given time, the turbine is in one of these two discrete states, with an "up" status occurring with probability p and a "down" status with probability $1-p$. The parameter p, representing the turbine's reliability, reflects the likelihood of the turbine being operational during a given time frame. Although reliability typically varies over time, for this analysis, we treat p as constant. This assumption holds when the evaluation time frame is fixed; for instance, when considering the annual energy output, using the turbine's operational probability over a year is reasonable. This approach aligns with the standard practice of collecting wind speed data over one-year intervals. Furthermore, p can be interpreted as the long-term or limiting reliability of the turbine. Thus, within the scope of this study, we address a static reliability problem.

Remark: [12] discussed the following properties of the distribution of the wind turbines power. According to this study, the total power generated by the whole plant is presented as $\mathcal{P}_N = h\big(U(t), \boldsymbol{V}(t)\big)$, for some function h, where $U(t)$ represents the stochastic process characterizing wind speed, while $\boldsymbol{V}(t) = \big(V_1(t), \cdots, V_N(t)\big)$ is a vector of turbines' that encapsulates the operational states of the turbines at a given time t. Specifically, $V_i(t)$=1 if the ith turbine is operational at time t and $V_i(t)$=0 if it is not functioning. If the failure time of the ith turbine is represented by F_i, then $P(V_i(t)=1) = P(F_i > t) = p(t), i = 1,2,\cdots,N$. That is, in the present study $\mathcal{P}_N = h\big(U(t), \boldsymbol{V}(t)\big)$ where $\boldsymbol{V} = (V_1, \cdots, V_N)$, and $\mathrm{P}(V_i = 1) = p, i = 1,2,\cdots,N$.

In a wind farm comprising N independent and identical wind turbines, the CDF of the total power output can be determined using

$$P(\mathcal{P}_N \le t) = \sum_{j=0}^{N} \binom{N}{j} p^j (1-p)^{N-1}\, \theta_j(t) \qquad (7)$$

where

$$\theta_j(t) = \begin{cases} 0, & \text{if } t < 0 \\ \gamma_j(t) & \text{if } 0 \le t < j\,\mathcal{P}_{rt} \\ 1 & \text{if } t \ge j\mathcal{P}_{rt} \end{cases} \qquad (8)$$

with

$$\gamma_j(t) = 1 - F(u_{\text{off}}) + F\left(\left[\frac{t}{j\mathcal{P}_{rt}}(u_{\text{rt}}^3 - u_{on}^3) + u_{on}^3\right]^{\frac{1}{3}}\right) \qquad (9)$$

In equation (7), p denotes the probability that turbine is operational. The CDF of the power generated by a single wind turbine is

$$\theta(t;p) = \begin{cases} 0, & \text{if } t < 0 \\ p\theta(t) + 1 - p & \text{if } 0 \le t < \mathcal{P}_{rt} \\ 1 & \text{if } t \ge \mathcal{P}_{rt} \end{cases}$$

Similarly, PDF of the power generated by a single wind turbine is

$$\varphi(t;p) = p\theta_1(t) + (p[F(u_{\text{on}}) + 1 - F(u_{\text{off}})] + 1 - p)\delta(t)\; p[F(u_{\text{off}}) - F(u_{\text{rt}})]\delta(t - \mathcal{P}_{rt})$$

where $\delta(t)$ is the Dirac's delta function.

The mean output when a unit is available can be determined from

$$\mu_1 = p\left[\int_0^{\mathcal{P}_{rt}} t\theta_1(t)dt + \mathcal{P}_{rt}[F(u_{\text{off}}) - F(u_{\text{rt}})]\right]$$

In a wind energy facility comprising N identical turbines, the average power output produced by the entire plant is represented by $\mu_N = N\mu_1$.

The scenario involving a fleet of nonidentical wind turbines is of significant practical interest. Wind turbine heterogeneity can be distinguished in two key cases. In the first case, turbines exhibit varying reliability metrics while maintaining identical performance characteristics, such as rated power. This situation commonly occurs when turbines with equivalent specifications are sourced from different manufacturers. The second case involves variation in both reliability metrics and operational characteristics across the turbine fleet. For analysis, we assume turbines with diverse reliability values, denoted as p_j for the j-th turbine. We have

$$P(\mathcal{P}_N \le t) = \sum_{j=0}^{N} P(\omega_N = j)\, \theta_j(t),$$

where the probability $P(\omega_N = j)$ can be recursively obtained from $P(\omega_N = j) = P(\omega_{N-1} = j-1)p_N + P(\omega_{N-1} = j)(1-p_N)$, for $0 < j < N$, with $P(\omega_N = 0) = \prod_{j=1}^{N}(1-p_j)$ and $P(\omega_N = N) = \prod_{\mathrm{j}=1}^{N} p_j$ [9].

4. Applications and numerical results

In this section, we compare the wind power distribution presented in [12] using three distinct probability distributions: Weibull, Birnbaum-Saunders (BS), and gamma distributions. Accurate modeling of wind power generation requires an appropriate probability distribution for wind speed, in conjunction with the specific characteristics of the wind turbine. The wind speed distribution is defined by $F(v) = P(V \le v)$, where V is the wind speed, while the turbine parameters u_{off}, u_{on}, u_{rt} and $\mathcal{P}_{rt}$ are specified by the manufacturer.

[19] conducted a comprehensive analysis of wind speed data in the Alaçatı region of Çeşme, İzmir, Turkey, employing a two-parameter Weibull distribution as described by equations (3) and (4). Their findings indicate that the Weibull distribution provides a good fit for wind speed measurements taken at a height of 70 m. The estimated distribution parameters are a shape

parameter k =2.05 and a scale parameter σ=9.16. Consequently, based on their analysis, wind speed in this region can be effectively represented by the following Weibull PDF

$$f(u) = \left(\frac{2.05}{9.16}\right)\left(\frac{u}{9.16}\right)^{1.05} e^{-\left(\frac{u}{9.16}\right)^{2.05}}.$$

[10] studied the fit of the BS distribution to wind speed data collected from Canada. According to their results, the BS distribution was found suitable for modeling wind speed data. They estimated the unknown parameters in equation (5) as $\hat{\varrho} = 3.7887$ and $\hat{\varsigma} = 0.6127$. Consequently, based on their analysis, wind speed in this region can be effectively represented by the BS probability distribution function

$$F(u) = \Phi\left[\frac{1}{3.7887}\left\{\left(\frac{u}{0.6127}\right)^{\frac{1}{2}} - \left(\frac{0.6127}{u}\right)^{\frac{1}{2}}\right\}\right].$$

Lastly, [9] studied the fit of 2 parameters gamma distribution to wind speed data collected from Canada and according to their results, gamma distribution was found to be suitable for modeling wind speed data. They have estimated the unknown parameters in (6) as $\hat{\alpha} = 1.489$ and $\hat{\theta} = 1.605$. Consequently, based on their analysis, wind speed in this region can be effectively represented by the BS probability distribution function $F(u) = \frac{1}{\Gamma(1.489)1.605^{1.489}} u^{0.489} e^{-u/1.605}$.

In our comparisons we assume that NORDEX N50/800 wind turbine model with rated power of 800 kW, switch-on wind speed $u_{\text{on}} = 3m/s$, rated wind speed $u_{\text{rt}} = 15m/s$, and shut-off wind speed $u_{\text{off}} = 25m/s$, then from (8) and (9) the CDF of the real power generated by a single wind turbine is found to be

$$\theta(t;p) = \begin{cases} 0, & \text{if } t < 0 \\ p\theta(t) + 1 - p & \text{if } 0 \le t < 800 \\ 1 & \text{if } t \ge 800 \end{cases}$$

where

$$\theta(t) = 1 - e^{-\frac{1}{9.16^{2.05}}\left[\frac{t}{800}(15^3-3^3)+3^3\right]^{\frac{2.05}{3}}} + e^{-\left(\frac{25}{9.16}\right)^{2.05}}$$ for Weibull distribution,

$$\theta(t) = 1 - \Phi\left[\frac{1}{3.7887}\left\{\left(\frac{25}{0.6127}\right)^{\frac{1}{2}} - \left(\frac{0.6127}{25}\right)^{\frac{1}{2}}\right\}\right] +$$
$$\Phi\left[\frac{1}{3.7887}\left\{\left(\frac{\left[\frac{t}{800}(15^3-3^3)+3^3\right]^{\frac{1}{3}}}{0.6127}\right)^{\frac{1}{2}} - \left(\frac{0.6127}{\left[\frac{t}{800}(15^3-3^3)+3^3\right]^{\frac{1}{3}}}\right)^{\frac{1}{2}}\right\}\right]$$

for BS distribution and

$$\theta(t) = 1 - \frac{1}{\Gamma(1.489)1.605^{1.489}} 25^{0.489} e^{-25/1.605} +$$
$$\frac{1}{\Gamma(1.489)1.605^{1.489}}\left[\frac{t}{800}(15^3 - 3^3) + 3^3\right]^{\frac{0.489}{3}} e^{-\left[\frac{t}{800}(15^3-3^3)+3^3\right]^{\frac{1}{3}}/1.605}$$

for gamma distribution.

Figure 2 plots the CDF of total plant power, $F_{\mathcal{P}}(c_0)=P\{\mathcal{P}_N \le c_0\}$, for a farm of $N = 10$ identical turbines operating with availability $p = 0.9$. Here, c_0 denotes plant power threshold for reliability check. The three curves correspond to the same turbine power curve and availability model but different wind-speed laws fitted for the site: Weibull ($k = 2.05, \lambda = 9.16$), Gamma ($\eta = 5.523, \theta = 1.422$), and BS ($\alpha = 3.7887, \beta = 0.6127$). Because these are CDFs, a left-shifted curve implies more probability mass at lower plant outputs (more conservative for exceedance targets), while a right-shifted curve implies more mass at higher outputs. The changes in slope around the middle of the plot reflect many turbines entering the rated-power segment of the power curve; small step-like features come from the discrete convolution used to obtain the plant PMF.

According to Figure 2, the BS (green) curve is the leftmost across the 1-8 MW range, reaching high CDF values at relatively small c_0. It therefore predicts a larger probability of being below a given capacity threshold, i.e., most conservative for sizing by exceedance: for a target $P\{\mathcal{P}_N > c_0\} \ge p_0$, it will typically require the largest N. In this inequality, p_0 dnotes the target exceedance probability at c_0. The Weibull (blue) curve is the rightmost, implying more mass at higher outputs and thus the most optimistic sizing (smallest N) under the same target. The Gamma (orange) curve sits between Weibull and BS, providing an intermediate assessment of risk and required fleet size. Differences among the laws are largest in the mid-range of outputs (roughly 2-7 MW here), precisely where practical capacity thresholds c_0 often lie; the curves nearly coincide only near the upper tail where $F(x) \to 1$.

Figure 3 repeats the plant-power CDF comparison for the same wind-speed laws as in Figure 2, Weibull ($k = 2.05, \lambda = 9.16$), Gamma ($\eta = 5.523, \theta = 1.422$), and Birnbaum-Saunders ($\alpha = 3.7887, \beta = 0.6127$) but with higher availability $p = 0.98$ for each of the N =10 turbines. As before, a curve farther to the right implies a greater probability of achieving higher plant outputs (more optimistic for exceedance targets), while a curve to the left is more conservative.

If we compare Figures 2 and 3, one can easily conclude that raising availability from p=0.90 to p=0.98 shifts all three CDFs to the right, indicating higher achievable outputs across the board and smaller shortfall risk for any fixed capacity threshold c_0. The BS curve (green) stays the leftmost over the practical range (≈2-8 MW), thus remaining the most conservative law for exceedance-based sizing; it would typically prescribe the largest N to satisfy $P\{\mathcal{P}_N > c_0\} \ge p_0$. The Gamma curve (orange) is now slightly to the right of Weibull (blue)

through the mid-slope region, i.e., it is a bit more optimistic than Weibull in predicting higher outputs for the same c_0. The gap between Gamma and Weibull, however, is small compared with their separation from BS. At this higher availability, the differences among laws shrink, especially in the upper tail where all three CDFs approach 1 near the farm's aggregate rated power. Consequently, the sensitivity of N to the choice of wind-speed law is lower at p=0.98 than at p=0.90, though BS still yields the largest N.

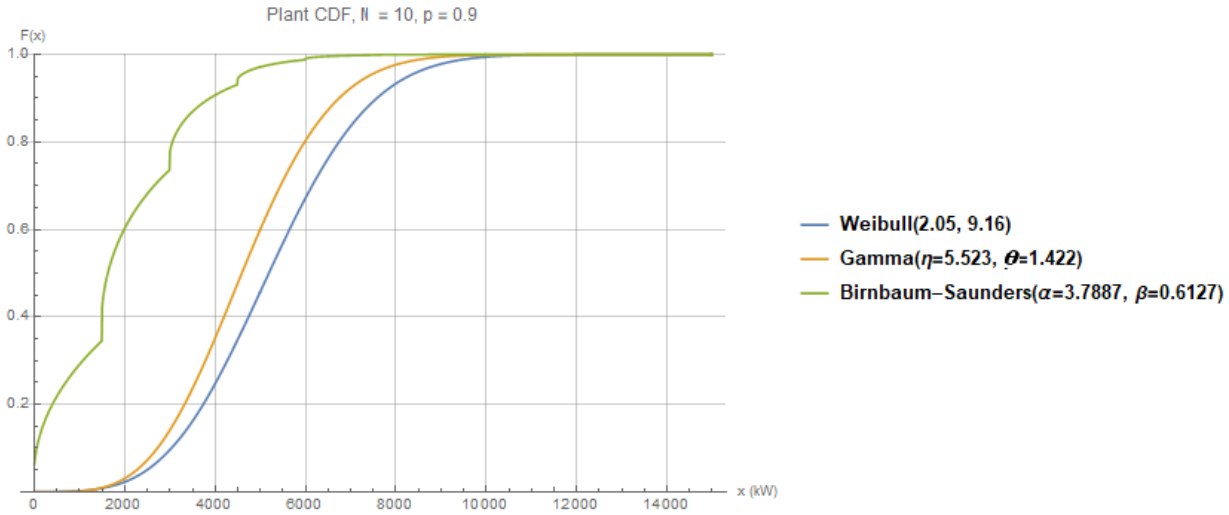

Figure 2. Comparison of the CDF of the wind plant power for N = 10 and p=0.9.

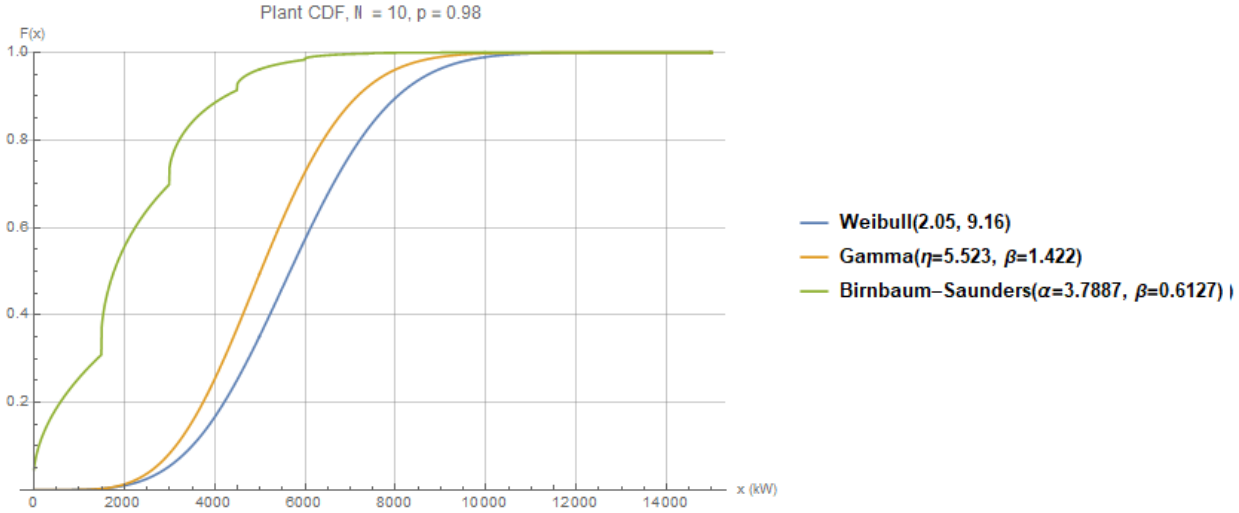

Figure 3. Comparison of the CDF of the wind plant power for N = 10 and p=0

Table 1.Comparison of cumulative probabilities for the wind plant power for p=0.9.

	N = 3			N = 5			N = 10		
c_0 (kW)	Weibull	Gamma	BS	Weibull	Gamma	BS	Weibull	Gamma	BS
100	0.0313	0.0174	0.5379	0.0024	0.0008	0.3534	2.4812×10^{-6}	1.6927×10^{-7}	0.1213
300	0.0907	0.0771	0.6084	0.0122	0.0072	0.4326	0.0000	7.4150×10^{-6}	0.1792
500	0.1561	0.1595	0.6476	0.0292	0.0239	0.4795	0.0002	0.0001	0.2191
800	0.2546	0.2935	0.6872	0.0662	0.07	0.5288	0.001	0.0006	0.2655
1000	0.3172	0.3784	0.7071	0.0968	0.1128	0.5545	0.0021	0.0016	0.2914
1500	0.4735	0.5621	0.9022	0.1874	0.2441	0.7555	0.0085	0.0095	0.4218

Table 1 reports, for a set of power thresholds c_0 (100-1500 kW), the probability that the total plant output is at or below c_0 when turbine availability is p=0.90. Results are shown for three fleet sizes N={3,5,10} and three wind-speed models (Weibull, Gamma, Birnbaum-Saunders). Larger table entries mean higher chance of being below the threshold (i.e., more conservative from a capacity-assurance perspective). Comparing columns across N reveals how aggregation reduces the likelihood of very low output; comparing rows across the three laws shows the model sensitivity.

For small c_0 (e.g., 100–300 kW), BS produces markedly larger probabilities than Weibull/Gamma, especially at N=10 (e.g., at x=100: BS 0.1213 vs. Weibull 2.5×10^{-6}, Gamma 1.7×10^{-7}). This indicates a heavier lower tail for BS in the plant-output distribution, i.e., it assigns much more mass to near-zero production events once availability is included. For Mid-range thresholds (500–1000 kW), across N, the ordering BS > Gamma > Weibull generally persists. BS remains the most conservative (highest $F_{\mathcal{P}}(c_0)$), Gamma sits in the middle, and Weibull is the least conservative (lowest $F_{\mathcal{P}}(c_0)$), implying the most optimistic plant throughput among the three. Holding c_0 fixed, increasing N decreases $F_{\mathcal{P}}(c_0)$ (e.g., at c_0 =800, BS: 0.6872→0.5288 from N=3 to 10). This is the expected aggregation effect: more turbines shift the plant output distribution rightward and reduce the probability of falling below a given threshold. Lastly, discrepancies between the laws remain visible even at c_0=1500: BS yields the highest probabilities, followed by Gamma, then Weibull (e.g., for N=10: BS 0.4218, Gamma 0.2191, Weibull 0.0085). Thus, conclusions about adequacy at "1 MW–class" thresholds are model-sensitive.

Table 2 discusses, for each mean-power requirement $c_0 \in${1200,1500,1800,2200} kW, the smallest fleet size N^* that satisfies $E(\mathcal{P}_N) \geq c_0$ and the corresponding achieved mean power. Results are shown for the three wind-speed models used throughout the paper (Weibull, Gamma, Birnbaum–Saunders). Reading down a column reveals how the sizing decision changes with the target m_0; reading across the "Law" rows at a fixed m_0 shows the model sensitivity of N. For every target c_0, the Weibull law requires the fewest turbines; Gamma is slightly more conservative; BS requires substantially more. The achieved mean power depends only on the chosen N (and the law), not on m_0 itself; as m_0 crosses a step, N increments and power "jumps." Sizing is highly model-sensitive. Unless the wind-speed law is well calibrated to site data, planners should report a range for N across plausible laws (e.g., c_0 =500, c_0 =1500: $N\in${3,4,8}) and assess cost/risk trade-offs accordingly.

Table 2. Comparison of the mean power

Law	c_0 (kW)	N^*	achieved mean power kW)
Weibull	1200	3	1569.44
Gamma	1200	3	1393.08
BS	1200	7	1332.63
Weibull	1500	3	1569.44
Gamma	1500	4	1857.44
BS	1500	8	1523.01
Weibull	1800	4	2092.59
Gamma	1800	4	1857.44
BS	1800	10	1903.76
Weibull	2200	5	2615.74
Gamma	2200	5	2321.80
BS	2200	12	2284.51

Table 3 presents, for each target pair (c_0, p_0), the minimum number of identical turbines N^* required so that the plant meets the quantile requirement $P\{\mathcal{P}_N>c_0\} \geq p_0$. We compute N^* under three alternative wind-speed laws—Weibull, Gamma, and BS. Because N is integer-valued, the achieved probability $P(\mathcal{P}_N > c_0)$ is shown as well; it is the value obtained at that smallest feasible N and therefore (by construction) is just above the target p_0. According to this table, for the same performance target, the required fleet size N varies substantially across the three laws. For example, at $(c_0 = 800, p_0 = 0.90)$, Weibull needs 5 turbines (achieved 0.934), Gamma needs 5 (0.930), while BS needs 17 (0.905).

Table 3. Optimal Turbine Count (N) and Achieved Exceedance Probability $P(>c_0)$ under Weibull, Gamma, and BS Models at Selected Targets (c_0, p_0)

c_0 (kW)	p_0	Weibull N^*	Weibull achieved $P(\mathcal{P}_N>c_0)$	Gamma N^*	Gamma achieved $P(\mathcal{P}_N>c_0)$	BS N^*	BS achieved $P(\mathcal{P}_N>c_0)$
800	0.70	3	0.745442	3	0.706534	10	0.734498
800	0.80	4	0.866604	4	0.849658	12	0.800832
800	0.90	5	0.933844	5	0.929981	17	0.905316
800	0.95	6	0.969021	6	0.969899	22	0.956347
1000	0.70	3	0.770984	4	0.715529	10	0.708562
1000	0.80	4	0.819115	5	0.887164	13	0.805908
1000	0.90	5	0.903215	6	0.945696	17	0.904202
1000	0.95	6	0.950904	7	0.975616	23	0.954138
1200	0.70	4	0.770984	4	0.715529	11	0.722657
1200	0.80	5	0.869096	5	0.837594	14	0.812002

For the lower threshold c_0=800 kW, both laws yield the same N^* across all p_0 levels; Weibull's achieved probability is slightly higher but very close to Gamma's. Across all (c_0, p_0) pairs, BS requires many more turbines than Weibull or Gamma to reach the same reliability target. If BS is used for planning, the plant will be over-built relative to the other two models, yielding larger safety margins and higher capex. For a fixed distribution, N^* increases as the target becomes more demanding-either higher c_0 or higher p_0. The achieved probabilities exceed p_0 by a small buffer (typically 0.01-0.07), which is the natural result of optimizing over an integer N^*. Finally, if the location's wind regime is closer to a Weibull or Gamma fit, using BS could materially inflate the required fleet size. Conversely, if a very conservative design is desired (e.g., to hedge distributional misspecification), BS provides a built-in buffer.

These numerical findings can be explained by fundamental differences in the statistical properties of the three distributions. The Birnbaum-Saunders distribution exhibits a heavier lower tail compared to Weibull and Gamma, allocating more probability mass to low wind speeds. When these wind speeds are transformed through the cubic power curve, this lower-tail behavior translates to higher probabilities of low power output, yielding conservative sizing estimates. Conversely, the Weibull distribution's lighter lower tail and relatively heavier upper tail predict higher power outputs more frequently. The Gamma distribution, with its intermediate tail behavior, produces predictions between the two extremes. This tail behavior is visually evident in Figures 2 and 3, where the BS curve consistently remains leftmost across the 2-7 MW range. These distributional differences are amplified during the discrete convolution process that aggregates N turbines, particularly affecting exceedance probabilities at moderate capacity thresholds where the distributions exhibit maximum separation.

5. Limitations and Future Work

The present paper operates under several simplifying assumptions that warrant discussion. First, we assume spatial and temporal independence of both wind speeds and turbine failures. In reality, adjacent turbines experience correlated wind fields, and wake effects reduce downstream turbine performance-effects not captured in our model. Second, we employ parametric distributions fitted from published studies rather than site-specific empirical data, which may not fully represent local wind regime complexities such as diurnal patterns or seasonal variations.

Third, our analysis uses a single turbine model with fixed availability (p), whereas actual turbines exhibit time-varying reliability influenced by age, maintenance, and operating conditions. Future research should address these limitations by: (i) incorporating spatial correlation structures and wake models into the aggregation framework; (ii) validating predictions against long-term power generation data from operational wind farms; (iii) extending the comparison to additional distributions (e.g., mixtures, generalized distributions) and multiple turbine technologies; and (iv) integrating time-series models that capture temporal correlation and non-stationarity in wind regimes. Such extensions would enhance the practical applicability of distributional comparisons for site-specific planning and operational decision-making.

6. Conclusion

We compared three wind-speed laws Weibull, Gamma, and BS within a unified wind-plant sizing framework. For a target threshold c_0 and an exceedance requirement p_0, we computed the minimum number of identical turbines N^* such that $P\{\mathcal{P}_N > c_0\} \geq p_0$, using a realistic turbine power curve (cut-in, rated, and cut-out) and an explicit per-turbine availability p. Because procedures were held constant across models, differences trace directly to the wind-speed distribution. Across all (c_0, p_0) evaluated, Weibull yielded the smallest N^*, BS the largest N^*, and the Gamma lay between; the gaps widened at higher reliability targets (larger p_0) and as c_0 moved deeper into the upper tail.

At p_0 levels (e.g., 0.90-0.95), BS often requires substantially more turbines than Weibull. Achieved exceedance probabilities at the reported N^* matched or exceeded p_0, confirming a well-calibrated search. Practically, the choice of wind-speed model materially affects sizing: when shortfall costs are high, BS (or at least reporting BS-based N^*) provides a risk-averse benchmark, while Weibull can understate the count needed to exceed c_0 reliably. We recommend reporting a distribution-aware range [N^*_{Weibull}, N^*_{Gamma}, N^*_{BS}] with the achieved $P\{\mathcal{P}_N > c_0\}$. Sensitivity to p, c_0, and p_0 was monotone and qualitatively consistent across models, with the largest magnitude of change under BS.

7. References

[1] Zárate-Miñano, R., Anghel, M. ve Milano, F., "Continuous Wind Speed Models Based on Stochastic Differential Equations", Applied Energy, 104, 42–49, 2013.

[2] Louie H, Sloughter JM. Probabilistic modeling and statistical characteristics of aggregate wind power. Large Scale Renewable Power Generation, Green Energy and Technology. Springer Science+Business Media Singapore; 2014. p. 19–51.

[3] Li, P., Guan, X. ve Wu, J., "Aggregated Wind Power Generation Probabilistic Forecasting Based on Particle Filter", Energy Conversion and Management, 32, 96–579, 2015.

[4] Xydas, E., Qadrdan, M., Marmaras, C., Cipcigan, L., Jenkins, N., ve Ameli, H., "Probabilistic Wind Power Forecasting and Its Application in the Scheduling of Gas-Fired Generators", Applied Energy, 32, 192–382, 2017.

[5] Olaofe, Z. O. ve Folly, K. A., "Wind Power Estimation Using Recurrent Neural Network Technique", IEEE Power and Energy Society Conference and Exposition in Africa: Intelligent Grid Integration of Renewable Energy Resources (PowerAfrica), Johannesburg, South Africa, 1–7, 2012.
[6] Safari, B., "Modeling Wind Speed and Wind Power Distributions in Rwanda", Renewable and Sustainable Energy Reviews, 32, 15–925, 2011.
[7] Masseran, N., Razali, A. M., ve Ibrahim, K., "An Analysis of Wind Power Density Derived from Several Wind Speed Density Functions: The Regional Assessment on Wind Power in Malaysia", Renewable and Sustainable Energy Reviews, 32, 16–6476, 2012.
[8] Zhang, Y., Wang, J., ve Luo, X., "Probabilistic Wind Power Forecasting Based on Logarithmic Transformation and Boundary Kernel", Energy Conversion and Management, 32, 96–440, 2015.
[9] Sohoni, V., Gupta, S. ve Nema, R., "A Comparative Analysis of Wind Speed Probability Distributions for Wind Power Assessment of Four Sites", Turkish Journal of Electrical Engineering and Computer Sciences, 24(6), 4724–4735, 2016.
[10] Mohammadi, K., Alavi, O. ve McGowan, J. G., "Use of Birnbaum–Saunders Distribution for Estimating Wind Speed and Wind Power Probability Distributions", Energy Conversion and Management, 32, 109–143, 2017.
[11] Altunkaynak, A., Erdik, T., Dabanlı, İ., ve Şen, Z., "Theoretical Derivation of Wind Power Probability Distribution Function and Applications", Applied Energy, 32, 92–809, 2012.
[12] Eryilmaz, S., ve Devrim, Y., "Theoretical Derivation of Wind Plant Power Distribution with the Consideration of Wind Turbine Reliability", Reliability Engineering & System Safety, 185, 192–197, 2019.
[13] El Kihel, F., Baïda, M., El Khoukhi, H. ve El Hami, K., " Enhanced Weibull parameter estimation methods under complex terrain conditions", Renewable Energy, 223, 1190–1203, 2024.
[14] Hassan, L., Tavana, M. R. ve Khorram, E., "A neutrosophic BirnbaumSaunders distribution model for imprecise wind data", Energy Reports, 11, 347–359, 2024.
[15] Zhan, Y., Liu, S. ve Li, C., "Multifractal detrended fluctuation analysis and probabilistic distribution modeling of wind speed in Sichuan Province", Scientific Reports, 15 (2034), 1–13, 2025.
[16] Ndeba, A., Louafi, R. E. ve Benjha, T., "Characterization of wind speed distribution using the Champernowne model: Application to Green Energy Park, Ben Guerir", International Journal of Energy Research, 49 (7), 8259–8275, 2025.
[17] Phan, N., Vo, T. ve Nguyen, L., "Probabilistic models for wind speed prediction and strategic planning of wind energy in Vietnam", International Journal of Electrical and Electronics Engineering, 12 (1), 20–29, 2025.
[18] Bousla, H., El Boussaad, I. ve Bekka, A., "Weibull-based approaches for wind energy prediction: Comparative assessment and validation", Energy Procedia, 276, 530–540, 2025.
[19] Özay, C. ve Çeliktaş, M. S., "Statistical Analysis of Wind Speed Using Two-Parameter Weibull Distribution in Alaçatı Region", Energy Conversion and Management, 32, 121–149,2016.